PAPER • OPEN ACCESS

Photogrammetry and Remote Sensing for the identification and characterization of trees in urban areas.

To cite this article: Md Abdul Mueed Choudhury *et al* 2019 *J. Phys.: Conf. Ser.* **1249** 012008

IOP Conf. Series: Journal of Physics: Conf. Series **1249** (2019) 012008 doi:10.1088/1742-6596/1249/1/012008

Photogrammetry and Remote Sensing for the identification and characterization of trees in urban areas.

Md Abdul Mueed Choudhury[1], Sofia Costanzini[2], Francesca Despini[2], Paolo Rossi[2], Andrea Galli[1], Ernesto Marcheggiani[1,3], Sergio Teggi[2]

[1] Department of Agricultural, Food and Environmental Sciences, Marche Polytechnic University, Italy

[2] Department of Engineering Enzo Ferrari, University of Modena and Reggio Emilia, Italy

[3] Department of Earth and Environmental Sciences, University of Leuven, Belgium

Abstract. For the last few decades, there have been a lot of studies recognising the significant roles of the urban trees as a high-quality carbon sink. This work is a preliminary study about how remote sensing and photogrammetry could be useful tools to identify urban trees for the purpose of Carbon Storage (CS) computation in urban areas. Our first study area is a typical urban park located in Sassuolo, a municipality in the northern part of Italy in the so-called "Pianura Padana". We measured the tree Height (H) and the Diameter at Breast Height (DBH), required for the calibration of the CS, based on the tree allometry during the field data collection along with the constructing a 3D model through the photogrammetric approach. A high-resolution WorldView (WV) 3 satellite image of the same area, was classified using an object-oriented approach to count the number of trees varied with different species. This preliminary study will enhance the possibilities of the application of these approaches in case of the larger urban areas to ascertain the accuracy of the tree CS calibration.

1. Introduction

The world has been experiencing the fast-flowing and heedless urbanisation for the last few decades. Green infrastructures, as well as urban trees, have a significant impact on the atmospheric Carbon Storage (CS) and sequestration.

Recent studies suggest that the urban trees are not only being considered as an essential element for the climate change mitigation policies but also appreciated as a high-quality carbon sink for capturing the atmospheric Carbon dioxide (CO_2) to a significant level [1-2]. Exploring the information on the tree structure and species in urban areas with higher accuracy is substantial to predict the carbon stock and to improve the urban ecological services [3-4]. Satellite remote sensing has been widely used for tree characterisation and classification for the last few decades [5-11]. Even in the case of the urban trees, high spatial resolution satellite imagery has been utilised to identify the species along with the individual tree crown extraction [12-23].

In this study, we performed a preliminary analysis of urban trees by using remote sensing data combined with ground truth measurement. We used a high-resolution WorldView (WV) 3 image data providing eight multispectral bands along with the short-wave infrared (SWIR) bands which make it far better than the traditional four-band IKONOS and QuickBird data in case of the vegetation analysis [12]. In fact, urban tree classification with higher accuracy is still a considerable challenge, most studies recommend the application of the Object Based Image Analysis (OBIA) approach to improve the classification accuracy in urban areas [24-27]. We also utilised the OBIA approach as our goal was to classify and count the trees of different species required for the further CS calibration.

A photogrammetric approach was introduced to measure the tree height (H) [28] and during the field survey trunk Diameter at Breast Height (DBH) measurement along with the species identification was done. These tree parameters (H, DBH) were necessary also for the future estimation of the tree CS. Lidar and 3D reconstruction techniques are often applied in vegetation\forestry investigation [29-32].

In this study, a terrestrial photogrammetric approach was used to produce accurate point cloud. Lidar and aerial photogrammetry are expensive and are always applied for the detection of the large land areas. Terrestrial photogrammetry, such as small UAV photogrammetry, can be quickly implemented in urban areas for the detection of a small portion or of a single tree. Modern photogrammetry takes the advantages of the Structure-from-Motion (SfM) algorithm that allows the 3D reconstruction from a series of high redundant images, acquired without any rigorous design. Even SfM with multi-view stereo-photogrammetry is considerably a new technique, still few studies are evident in case of the tree measurement especially the linear metrics such as the DBH, H, crown spread and also the stem radius [28, 30-32]. We found the photogrammetric approach including the 3D model construction from the 2D images [33], would be truly useful for the tree H measurement, especially for the urban areas.

This study will be quite noteworthy to go forward with the computation of the urban tree CS for the urban planners and researchers through the proper management of the urban vegetations.

2. Data

2.1. Study area

The first study area is the ‘Ducal park’ (44°32′32.82″N, 10°46′48.36″E), an urban park located in Sassuolo, province of Modena in the northern part of Italy. This area is included in the well-known ‘Pianura Padana’ region, an area with high pollution values due to a large number of industries and the geographical and climatologic characteristics (Figure 1). The total land area of the park is around 11.53 ha. The park is composed of different tree species whereas the dominants are the *Acer campestre, Quercus robur* and *Populus nigra.*

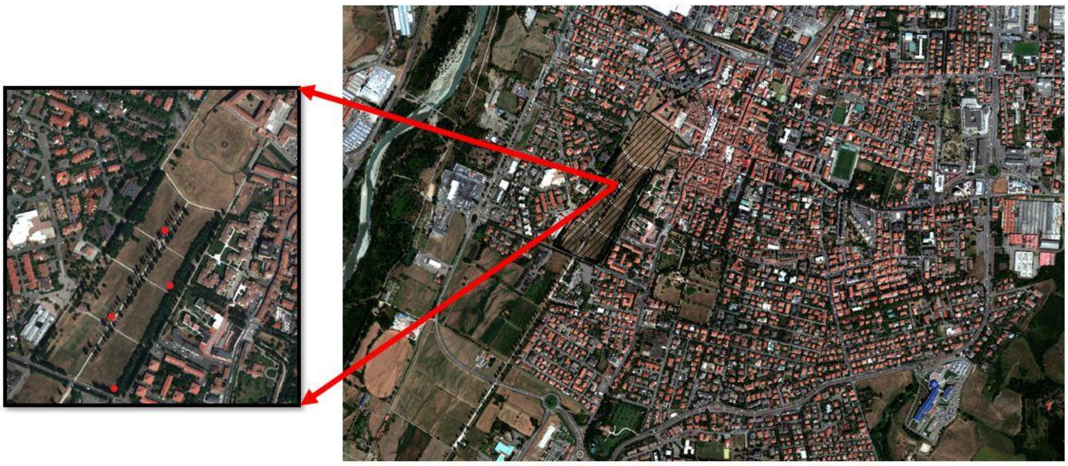

Figure 1. The study area in Sassuolo showing the sample plots (red circles) at the Ducal park.

2.2. Satellite image

The WV3 image data for this study was acquired on 31 July 2018 (Figure 2). The WV3 includes one panchromatic band of 0.3 m resolution and eight multispectral bands of 1.2 m resolution named:

- Coastal band (400–450 nm),
- Blue band (450–510 nm),
- Green band (510–580 nm),
- Yellow band (585–625 nm),
- Red band (630–690 nm),
- Red edge band (705–745 nm),
- NIR1 band (770–895 nm)
- NIR2 band (860–1040 nm) bands.

Having these additional four bands i.e. coastal, yellow, red-edge and NIR2, bring some advantage in case of the vegetation identification and analysis [12,42]. That is why WV3 image data was also preferred for the present study.

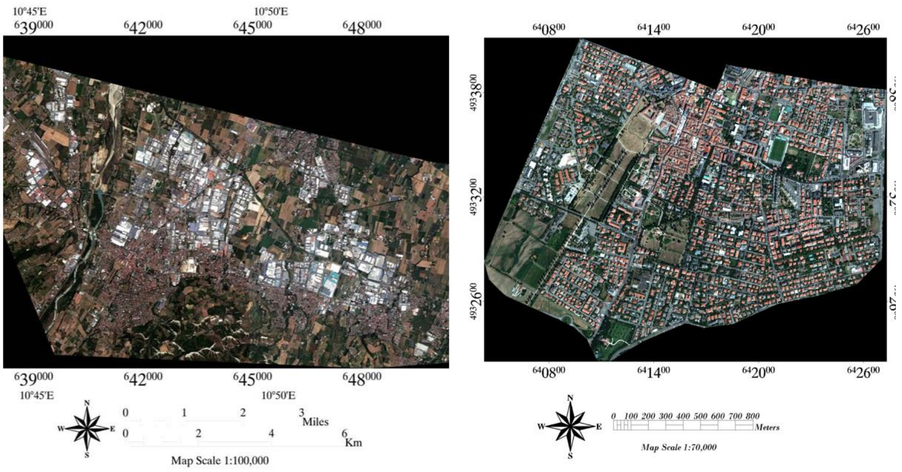

Figure 2. The WV3 image data (left) and the resized study region (right) considering the whole urban area.

2.3. Field data

Single tree location and measurements and image acquisition for the photogrammetry were carried out in the field in October 2018. Four plots were randomly selected in the park, and each of the plots had an area of 100m² (10m×10m). Each plot was composed of at least two trees of the same or different species. Field data such as the name of tree species and geographical coordinates of the trees were gathered along with the DBH. The total number of the three dominant trees in the park were also counted during the field survey. Having the tree positions recorded tree crowns were identified and delineated on the WV3 image. For the tree H measurement, 2D pictures were taken per plot utilising a hand-held digital camera considering the 3D model development through the SfM photogrammetric approach. Several pictures were acquired from different positions, recognizing the shorter to taller trees.

3. Methodology

3.1. Photogrammetric approach

Photogrammetric technique allows the 3D reconstructions of objects through the acquisition of 2D images, whereas in our case we produced the 3D model for each plot in order to measure the tree H along with the 3D model. The Agisoft PhotoScan(APS) software was utilized which implement the SfM algorithm[28,34]. All the trees were photographed placed in different sampling plots. The images were captured with a hand-held, digital SLR camera from photopoints at regular intervals around the perimeter of each plot. About 120-150 photos/plot were taken depending on the size of the trees. A semicircle pathway around each plot successively from the inner to outer part of the plot were followed to capture each image covering all the trees (Figure 3)

Figure 3. Dense point clouds of one of the investigated plots (APS model view), the blue squares represent the locations from which each of the images was taken.

The inner circle photos were taken from a distance having the tree-top, middle and bottom part of the tree, and the outer ones to have the whole tree within a frame. The SfM approach allows the 3D reconstruction from multiple images which ensures a high redundancy of images (each portion of the area of interest must be detected within 9-10 images at least). Also, a varying viewing geometry has to be guaranteed for obtaining accurate results. If no information about camera positions or point with known coordinates are added to the project, the reconstructed 3D point cloud will be generated within an arbitrary reference system lacking georeferencing and scale.

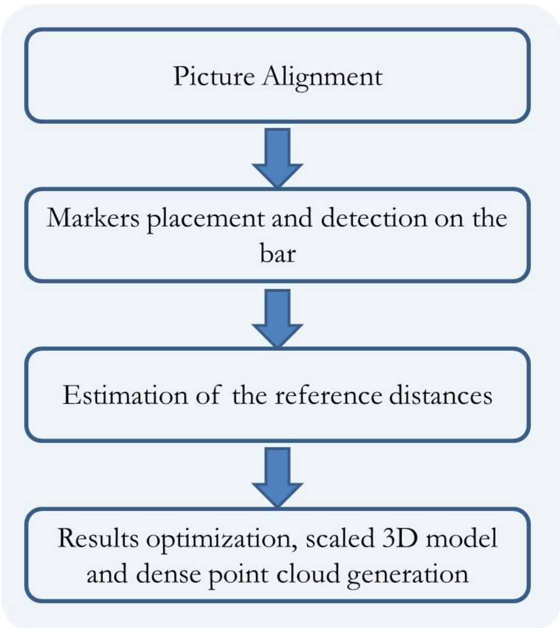

Figure 4. The flowchart of the H estimation through the SfM approach in APS.

In this case study, for measuring the tree H in the 3D model, a 4-meter graduated bar (Figure 4) was added to the area of interest as a reference. As the positioning of an object of known dimension allows the generation of scaled products that can be used for the measurement purpose [35], we were able to measure the tree H reconstructing the 3D model for each plot.

Figure 5. Photo of the graduated bar use as reference in the 3D reconstruction(a), view of the bar at the reconstructed 3D model in APS interface (b).

3.2. Remote sensing approach

3.2.1. Preprocessing Initially, the raw data had to be converted into surface reflectance. Thus, the conversion of the first digital number into the top of Atmosphere radiance was implied using sensor parameters. Before the processing and classifications, the atmospheric correction of the WV3 image was also done utilising the FLAASH plugin of the Environment for Visualizing Images (ENVI) software [50]. Then the image was resized by using the shapefile of the park.

3.2.2. Image segmentation and classification In urban areas, the traditional pixel-based image classification method usually shows a low classification accuracy due to high spectral variability within land cover classes that were affected by sun angle, gaps in tree canopies and shadows [45-46]. Considering these limitations, OBIA approach was introduced in this study to improve the classification accuracy [24-27, 53]. The OBIA method includes not only spectral information but also other added information such as context, texture, geometry and spatial features. [17,47], which can minimise the number of units to be considered for the classification [48]. The segmentation is the key procedure to divide the image into different significant objects where the spectral and spatial feature will be computed. The segmentation procedure divides the image into spatially continuous and homogeneous regions [49] and also limits the local spectral variation [24-25]. Here the Trimble eCognition Developer® 9 platform (Trimble, Munich, Germany) was utilised to employ the OBIA approach. Firstly, a multiresolution segmentation was performed where several attempts were done with the different values of the parameters to determine an adequate level of object recognition. An accurate segmentation is nothing but an essential prerequisite to ensure a significant classification. That is why those several attempts were necessary to attain the perfect combination of values of the parameters like scale, shape and compactness. Once I had the segmentation been done, I did move forward to the classification phase. The OBIA approach is also well-known for enhancing the advantages of spatial, spectral and texture information which is quite important for the classification. the Normalized Difference Vegetation Index (NDVI) was utilised to distinguish vegetated from non-vegetated objects [17,44].

The NDVI is a spectral vegetation index which has a significant correlation with the vegetation biomass [43]. It is the ratio of the reflectance in the Near Infrared band (ρ_{NIR}) and in the red band (ρ_{RED})'. The equation used to compute NDVI is:

$$NDVI = (\rho_{NIR} - \rho_{RED}) / (\rho_{NIR} - \rho_{RED}) \quad (1)$$

For the classification, the NDVI values were observed more than the 0.27 for all the vegetated areas whereas less than that value were found recognizing non-vegetated areas (i.e. Side-walks). The Forest Density Index (FDI), also known as the Forest Discrimination Index [51] was added which is a index computed using the reflectance in the NIR2 band (ρ_{NIR2}), in the red edge band ($\rho_{REDEDGE}$) and in the coastal band($\rho_{COASTAL}$):

$$FDI = \rho_{NIR2} - (\rho_{REDEDGE} + \rho_{COASTAL}) \quad (2)$$

This algorithm is useful to have a better recognition of vegetated and non-vegetated areas, even in case of the vegetation in the shadowed parts of the crowns. Having the vegetated areas well recognised, I did move on to the dominant tree species classification. At this stage, the Nearest Neighbor (NN) approach [52] was implied. For the classification training, about 30 samples of two dominant tree species were selected in the park including the *Quercus robur* and *Populus nigra* and the areas covered with grass. *Acer campestre* samples have not been selected because that species was always covered by *Quercus robur* crown. It is thus not possible to identify *Acer campestre* in this park from remote sensing due to overlapping questions. Along with the sample selection, the features had to be chosen for the NN approach. Different combinations of feature have been tested. Then looking at the computational time and output accuracy, the chosen features added were the layer means, standard deviation, pixel ratio, NDVI and FDI. From the classification output it is possible to determine the area for each of the tree species. By dividing this area with an average crown size for *Quercus robur* and *Populus nigra*, it was possible to have a first count of the number of trees. This approach will assist in classifying and counting the trees in case of the whole urban area for the calibration of the CS of urban trees.

4. Results and Discussion

4.1. 3D model reconstruction and H estimation

At the APS software, the 3D model for each plot was generated whereas in each model the reference scale bar was visible enough to validate our estimation (Figure 5). From the 3D model, H estimation was done by means of the scale tool available in APS software. Once the markers were placed on the APS software interface based on the scale bar, the software calibrated the distance among the markers (Figure 6). At least 2 to 3 reference markers of known distance were selected for each tree to ensure the higher accuracy of the tree H predictions. It was possible to evaluate the obtainable accuracy along the bar (as a local evaluation) but placing a marker at the tree top was difficult in case of the mixed canopies. So, later on I am going to introduce some tests to validate obtained results in a properly designed area in similar cases. The distance between the reference markers reported by the model is considered to verify the error of the model. The average error in case of the predicted distance was around 0.3 to 0.5 cm during the H calibration on the scale tool of the APS. The results show that the average H of the was so significant for each of the species. Unfortunately, there were a few studies on the urban tree H estimation utilising SfM approach on APS software, so I had to compare the results with the general European Forest Tree (EFT) database published in 2016 [36]. Even though this database was released based on the forestry areas, these results on urban trees were not so far different. For instance, for the three dominant species i.e. *Acer campestre, Quercus robur* and *Populus nigra* the estimated average heights were 10.18, 19.98 and 29.15 meters respectively (Table 1). Whereas according to the EFT database, the average height for the *Acer campestre* is typically 15 meters and for the *Quercus robur* and *Populus nigra* are 30 and 40 meters respectively [37-39]. Some other recent studies also estimated the average H 18.83 meters for the *Quercus robur* and for the *Populus nigra* the H was mentioned as 23±5 meters in Spain and Sweden respectively [40-41]. The differences among the resulted H of our trees and the H of the other studies are varied possibly due to the following reasons:

-Those studies were done in forestry areas in different environmental conditions;
-They utilised the traditional measurement methods;
-Those studies were implemented in case of the areas including a large number of trees.

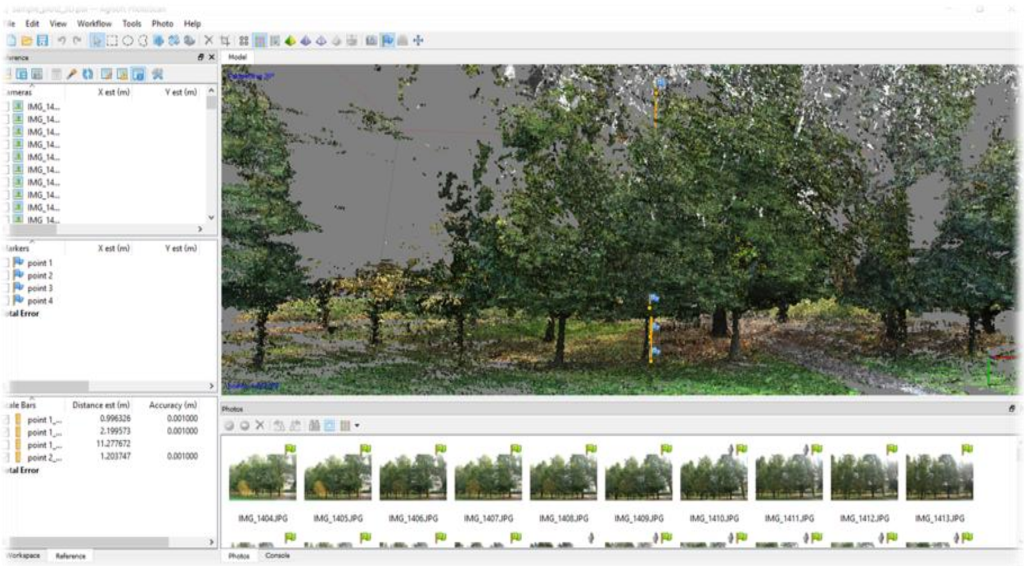

Figure 6. 3D model (Sample plot-1) with the estimated H at the scale tool(left) along with the blue markers on the bar in the APS interface.

Table 1. Estimated H of the trees in the sample plots including the mean height/species.

Sample plots	Tree species	Height (m)	Mean height/species(m)
1	*Acer campestre*	9	10.18
1	*Acer campestre*	11.5	
1	*Acer campestre*	9.8	
1	*Quercus robur*	17.6	19.98
1	*Quercus robur*	20.6	
2	*Acer campestre*	9.98	
2	*Acer campestre*	10.14	
2	*Acer campestre*	10.67	
2	*Quercus robur*	21.5	
2	*Quercus robur*	20.2	
3	*Populus nigra*	35.4	29.15
3	*Populus nigra*	29.3	
4	*Populus nigra*	28.3	
4	*Populus nigra*	23.6	

However, the method will be implied for the larger area considering the whole urban area as the SfM photogrammetric approach is found to be quite useful for the urban tree H measurement. This H measurement will be beneficial for the calibration and prediction of the total urban tree CS utilizing the tree allometry (Table 1).

4.2 WV3 image classification and tree counting

The result shows the classification was significant for the two considered species (Figure 7). In some cases, it was quite complex to extract the crowns of *Quercus robur* and *Populus nigra* in NN approach. That was observed due to having the similar spectral signatures for both of the species. Soon a separability analysis will be performed to evaluate if the spectral signature of the two species obtained by the WV3 data is enough to distinguish the two species. Finally, the number of trees were reckoned in case of the *Quercus robur* and *Populus nigra* based on mean crown area occupied by each of the species. We found 157 *Quercus robur* and 315 *Populus nigra* trees in the total park area. In field counting, 155 and 267 trees were identified for both of the species respectively. The difference between the tree populations in case of *Quercus robur* was convincing where the other was found to be more than the field counting. That might be happened due to the canopy type which led the problems during the classification. However, these results were pretty convincing which also recommend the possibilities to go on with the improvements considering the tree classification for the whole urban area. This kind of approach is so essential to estimate the tree biomass for mapping and to calibrate the tree CS in urban areas.

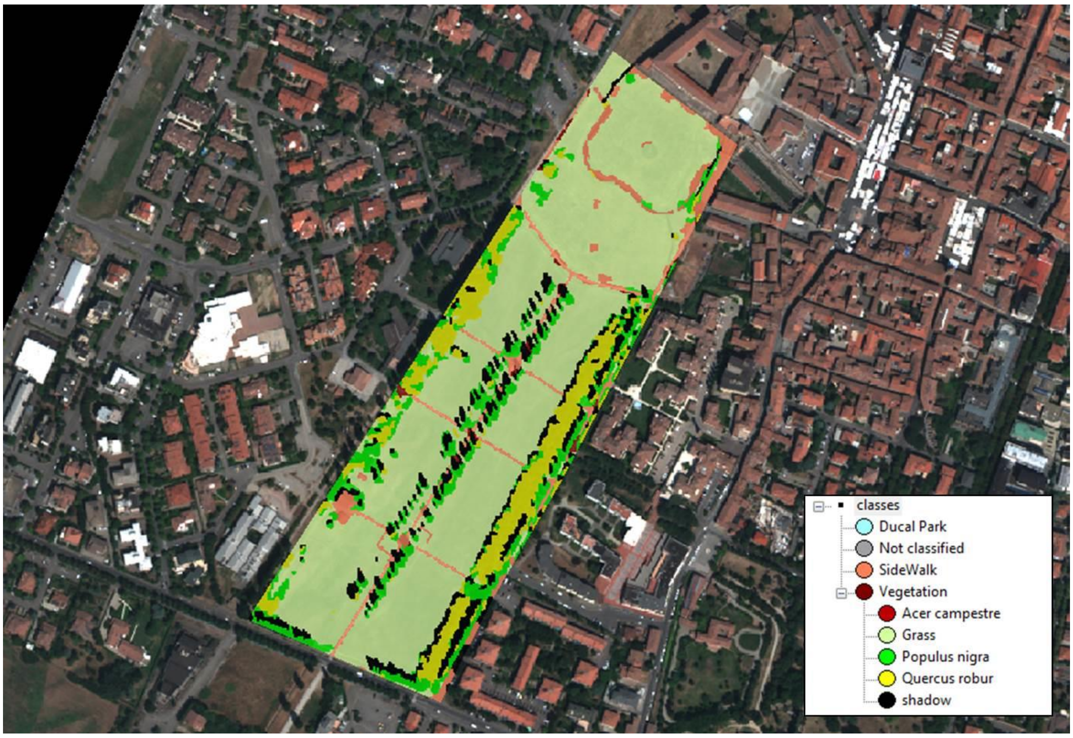

Figure 7. Object-Based Image Analysis (OBIA) Classification result with the Trimble eCognition Developer® 9.

5. Conclusion and future developments

This study was a preliminary effort to understand the potentiality of the photogrammetry and remote sensing tools to explore the information on urban tree structures and dominant species identification. This work represents the potential of high spatial resolution WV3 image data for detailed tree species mapping is promising. The future efforts will be done considering the whole urban area involving the refinement of the tree identification and segmentation, comparison and analysis of various algorithms for the automated identification of trees in mixed plots. In the case of photogrammetry, the result enhances the possibility of utilising the SfM approach for the calibration of urban tree Height (H) which is one of the significant tree inventories to estimate the tree CS. These approaches will be employed for further application correlating the WV3 image data and tree inventories to compute the urban tree Carbon Storage (CS). Once it is implemented in case of the whole urban area, the findings will provide an accurate and significant way to the city planners for recognising the level of tree CS, localised in different parts of the city.

References

[1] Davies Zoe G, Edmondson Jill L, Heinemeyer Andreas, Leake Jonathan R and Gaston Kevin J 2011 Mapping an urban ecosystem service: quantifying above-ground carbon storage at a city-wide scale *Journal of Applied Ecology* 2011, **48**, 1125–1134

[2] Godwin Christopher, Gang Chena, Kunwar K. Singh 2014 The impact of urban residential development patterns on forest carbon density: An integration of LiDAR, aerial photography and field mensuration *Landscape and Urban Planning* **136** (2015) 97–109

[3] Song C 2005 Spectral mixture analysis for subpixel vegetation fractions in the urban environment: How to incorporate endmember variability? *Remote Sensing of Environment*, **95**, 248–263

[4] Yang L, Xian G, Klaver J M & Deal B 2003 Urban lad-cover change detection through sub-pixel imperviousness mapping using remotely sensed data *Photogrammetric Engineering and Remote Sensing*, **69**, 1003–1010

[5] Pu R & Landry S 2012 A comparative analysis of high spatial resolution IKONOS and WorldView-2 imagery for mapping urban tree species *Remote Sensing of Environment* **124** (2012) 516–533

[6] Hájek F 2006 Object-oriented classification of Ikonos satellite data for the identification of tree species composition *Journal of Forest Science*, **52**(4), 181–187

[7] Ke Y, & Quackenbush L J 2007 Forest species classification and tree crown delineation using quickbird imagery ASPRS 2007, Annual Conference. Tampa, Florida, May 7-11, 2007

[8] Mora B, Wulder M A, & White J C 2010 Identifying leading species using tree crown metrics derived from very high spatial resolution imagery in a boreal forest environment *Canadian Journal of Remote Sensing*, **36**(4), 332–344

[9] Sugumaran R, Pavuluri M K, & Zerr D 2003 The use of high-resolution imagery for identification of urban climax forest species using traditional and rule-based classification approach *IEEE Transactions on Geoscience and Remote Sensing*, **41**(9),1933–1939

[10] Voss M & Sugumaran R 2008 Seasonal effect on tree species classification in an urban environment using hyperspectral data, LiDAR, and an object-oriented approach *Sensors*, **8**, 3020–3036

[11] Carleer A & Wolff E 2004 Exploitation of very high resolution satellite data for tree species identification *Photogrammetric Engineering and Remote Sensing*, **70**(1),135–140

[12] Dan Li, Yinghai Ke , Huili Gong and Xiaojuan Li 2015 Object-Based Urban Tree Species Classification Using Bi-Temporal WorldView-2 and WorldView-3 Images *Remote Sens*. 2015, **7**(12), 16917-16937

[13] Chao Yu, Mingyang Li, Mifang Zhang 2015 Classification of Dominant Tree Species in An Urban Forest Park Using the Remote Sensing Image of WorldView-2 8th International Congress on Image and Signal Processing (CISP 2015) https://ieeexplore.ieee.org/document/7407976 DOI: 10.1109/CISP.2015.7407976
[14] Katoh M 2004 Classifying tree species in a northern mixed forest using high-resolution IKONOS data Journal of Forest Research, 9, 7–14
[15] Kong C, Kai X & Wu C 2006 Classification and extraction of urban land-use information from high-resolution image based on object multi-features *Journal of China University of Geosciences*, **17**(2), 151–157
[16] Ikokou G B & Smith J 2013 A Technique for Optimal Selection of Segmentation Scale Parameters for Object-oriented Classification of Urban Scenes South African *Journal of Geomatics*, Vol. **2**, No. 4, August 2013 https://www.ajol.info/index.php/sajg/article/view/106976
[17] Shojanoori R, Shafri H Z M, Mansor S & Ismail M H 2016 The Use of WorldView-2 Satellite Data in Urban Tree Species Mapping by Object-Based Image Analysis Technique Sains Malaysiana 45(7) (2016): 1025–1034
[18] Adeline K R M, Briottet X, Paparoditis N & Gastellu-Etchegorry J P 2013 Material reflectance retrieval in urban tree shadows with physics-based empirical atmospheric correction IEEE Urban Remote Sensing Event (JURSE), São Paulo, Brazil, April 21-23
[19] Cho M A, Mathieu R, Asner G P , Naidoo L, Aardt J V, Ramoelo A, Debba P, Wessels K, Main R, Smit I P J & Erasmus B 2012 Mapping tree species composition in South African savannas using an integrated airborne spectral and LiDAR system *Remote Sens. Environ*. **125**: 214-226
[20] Forzieri G, Tanteri L, Moser G. & Catani F 2013 Mapping natural and urban environments using airborne multi-sensor ADS40–MIVIS–LiDAR synergies *Int. J. Appl. Earth ObsGeoinf*. **23**: 313-323
[21] Hao Z, Heng-Jia S & Bo-Chun Y 2011 Application of hyper spectral remote sensing for urban forestry monitoring in natural disaster zones. *IEEE International Conference on Computer and Management* (CAMAN). pp. 1-4
[22] Wania A & Weber C 2007 Hyperspectral imagery and urban green observation Urban Remote Sens Event (JURSE), Paris. pp. 1-8
[23] Zhang C & Qiu F 2012 Mapping individual tree species in an urban forest using airborne LiDAR data and hyperspectral imagery *Photogramm Eng Remote Sens*. **78**: 1079-1087
[24] Li C, Yin J & Zhao J 2010 Extraction of urban vegetation from high resolution remote sensing image International Conference on Computer Design and Applications (ICCDA) 4: 403-406
[25] Lobo A 1997 Image segmentation and discriminant analysis for the identification of land cover units in ecology *IEEE Trans Geosci. Remote Sens*. **35**: 1136-1145
[26] Puissant A, Rougier S & Stumpf A 2014 Object-oriented mapping of urban trees using Random Forest classifiers *International Journal of Applied Earth Observation and Geoinformation* **26**: 235-245
[27] Shouse M, Liang L & Fei S 2013 Identification of understory invasive exotic plants with remote sensing in urban forests. *International Journal of Applied Earth Observation and Geoinformation* **21**: 525-534
[28] Miller J, Morgenroth J & Gomez C 2015 3D modelling of individual trees using a handheld camera: Accuracy of height, diameter and volume estimates *Urban Forestry & Urban Greening* **14** (2015) 932–940
[29] Dandois J P, Ellis E C, 2013 High spatial resolution three-dimensional mapping of vegetation spectral dynamics using computer vision. *Remote Sens. Environ* **136**, 259–276
[30] Fritz A, Kattenborn T, Koch B 2013 UAV-based photogrammetric point clouds –tree stem mapping in open stands in comparison to terrestrial laser scanner point clouds *Int. Arch. Photogramm Remote Sens. Spat. Inf. Sci*. ISPRS Arch.XL-1/W2, 141–146.

[31] Liang X, Jaakkola A, Wang Y, Hyyppä J, Honkavaara E, Liu J, Kaartinen H 2014 The use of a hand-held camera for individual tree 3D mapping in forest sample plots *Remote Sens*. **6**, 6587
[32] Morgenroth J, Gomez C 2014 Assessment of tree structure using a 3D image analysis technique – a proof of concept Urban For. Urban Green
[33] De Eugenio A, Fernández-Landa A, Merino-de-Miguel S 2018 Modelos 3D derivados de fotogrametría terrestre para la estimación de variables de inventario forestal *Revsta de Teledetección Asociación Española de Teledetección* (2018) **51**, 113-124
[34] M J Westoby, J Brasington, N F Glasser, M J Hambrey, J M Reynolds 'Structure-from-Motion' photogrammetry: A low-cost, effective tool for geoscience applications *Geomorphology* **179** (2012) 300–314
[35] Castagnetti C, Rossi P & Capra A 2018 3D Reconstruction of rock paintings: a cost-effective approach based on modern photogrammetry for rapidly mapping archaeological findings In *IOP Conference Series: Materials Science and Engineering* (Vol. **364**, No. 1, p. 012020) IOP Publishing
[36] San-Miguel-Ayanz, J, de Rigo D, Caudullo G, Houston Durrant T, Mauri A (Eds.) 2016 European Atlas of Forest Tree Species Publication Office of the European Union, Luxembourg
[37] Zecchin B, Caudullo G, de Rigo D 2016 Acer campestre in Europe: distribution, habitat, usage and threats In: San-Miguel-Ayanz J, de Rigo D, Caudullo G, Houston Durrant T, Mauri A (Eds.), European Atlas of Forest Tree Species. Publ. Off. EU, Luxembourg, pp. e012c65+
[38] Eaton E, Caudullo G, Oliveira S, de Rigo D 2016 Quercus robur and Quercus petraea in Europe: distribution, habitat, usage and threats In: San-Miguel-Ayanz J, de Rigo D, Caudullo G, Houston Durrant T, Mauri A (Eds.) European Atlas of Forest Tree Species Publ. Off. EU, Luxembourg, pp. e01c6df+
[39] de Rigo D, Enescu C M, Houston Durrant T, Caudullo G, 2016 Populus nigra in Europe: distribution, habitat, usage and threats In: SanMiguel-Ayanz J, de Rigo D, Caudullo G, Houston Durrant T, Mauri A (Eds.) European Atlas of Forest Tree Species Publ. Off. EU, Luxembourg, pp. e0182a4+
[40] Miguel A Balboa-Murias, Alberto Rojo, Juan G Álvarez, Agustín Merino, 2006 Carbon and nutrient stocks in mature Quercus robur L. stands in *NW Spain Annals of Forest Science, Springer Verlag/EDP Sciences*, **63** (5), pp.557-565. <hal-00884009>
[41] Hjelm B, Mola-Yudego B, Dimitriou I & Johansson T 2015 Diameter–Height Models for Fast-growing Poplar Plantations on *Agricultural Land in Sweden BioEnergy Research*, **8**, 1759-1768
[42] Ibtisam Ab Majid, Zulkiflee Abd Latif and Nor Aizam Adnan 2016 Tree Species Classification Using Worldview-3 Data IEEE 7th Control and System Graduate Research Colloquium (ICSGRC 2016), 8 August 2016, UiTM Shah Alam, Malaysia
[43] K D Kanniah, N Muhamad and C S Kang 2014 Remote sensing assessment of carbon storage by urban *forest 8th International Symposium of the Digital Earth (ISDE8) IOP Conf. Series: Earth and Environmental Science* **18** (2014) 012151
[44] Mohammed H Obeyed, Yaseen T. Mustafa and Zeki M. Akrawee Estimating and Mapping Aboveground Biomass of Natural Quercus Aegilops Using WorldView-3 Imagery 2018 International Conference on Advanced Science and Engineering (ICOASE), Kurdistan Region, Iraq
[45] Johnson B & Xie Z 2013 Classifying a high resolution image of an urban area using super-object information *ISPRS Journal of Photogrammetry and Remote Sensing* **83**: 40-49
[46] Yu Q, Gong P, Clinton N, Biging G, Kelly M & Schirokauer D 2006 Object-based detailed vegetation classification with airborne high spatial resolution remote sensing imagery *Photogrammetric Engineering and Remote Sensing* **72**: 799-811
[47] Zhou W 2013 An object-based approach for urban land cover classification: Integrating LiDAR height and intensity data *IEEE Geoscience and Remote Sensing Letters* **10**(4): 928-931

[48] Youjing Z & Hengtong R 2007. Identification scales for urban vegetation classification using high spatial resolution satellite data In IEEE International Geoscience and Remote Sensing Symposium, (IGARSS), Barcelona, Spain. pp. 1472-1475

[49] Flanders D, Hall-Beyer M & Perverzoff J 2003 Preliminary evaluation of eCognition object based software for cut block delineation and feature extraction Canadian *Journal of Remote Sensing* **29**(4): 441-452

[50] Research Systems Inc. (RSI)ENVI user guide 2003

[51] Peter Bunting, Richard Lucas 2006 The delineation of tree crowns in Australian mixed species forests using hyperspectral Compact Airborne Spectrographic Imager (CASI) data. *Remote Sensing of Environment* Volume **101**, Issue 2, 30 March 2006, Pages 230-248

[52] Definiens AG 2005 eCognition Version 5 Object Oriented Image Analysis User Guide Munich, Germany

[53] Despini F., Teggi S (2012). Analysis of temperature maps of water bodies obtained from ASTER TIR images. *International Journal of Remote Sensing*, Volume **34,** Numbers 9-10 (May 2013), pp. 3636-3653;